Measurement of Polarity in Band-Limited Systems

3168 (K-2)

6M/K-2

D. B. (Don) Keele, Jr.
Audio Magazine, Hachette Magazines, Inc.
New York, NY 10019, USA

Techron, Div. Crown International, Inc.
Elkhart, IN 46517, USA

DBK Associates, Inc.
Elkhart, IN 46517, USA

Presented at the 91st Convention 1991 October 4–8 New York

AES

AN AUDIO ENGINEERING SOCIETY PREPRINT

Measurement of Polarity in Band-Limited Systems

D. B. (DON) KEELE, JR.

Audio Magazine, Hachette Magazines, Inc., New York, NY 10019, USA
Technon, Div. Crown International, Inc., Elkhart, IN 46517, USA
DBK Associates, Elkhart, IN 46517, USA

Polarity is usually measured by energizing the system under test with a wide-band asymmetrical test stimulus, such as a raised cosine pulse, and then observing the system's output on an oscilloscope. For a well-behaved flat-response minimum-phase system, such as an electronic device, the polarity determination is straightforward. However, for a general band-limited non-minimum-phase system with non-flat frequency response, such as a loudspeaker, the polarity assessment can be quite difficult due to waveform distortion.

A measurement method is presented that uses a narrow-band asymmetrical Hann-windowed tone burst, along with synchronous detection, to evaluate polarity at many points across a desired bandwidth. For a general system evaluated with tone bursts over a narrow frequency range, polarity is not just a simple two-valued function, but a continuum of values over the range of ±180°, that varies with frequency. A preliminary theory is presented that allows prediction of the tone-burst phase, and hence time-constrained narrow-band polarity (herein called polarity phase), from the system's conventional steady-state sinusoidal phase and group-delay responses.

0. INTRODUCTION

According to conventional polarity definition, a system that inverts polarity only (does no other processing other than polarity inversion), is defined as an operation that inverts the time waveform of the input signal $[f(t) \rightarrow -f(t)]$. In the frequency domain, a polarity reversal amounts to multiplying the spectrum of the input signal by an operator that rotates the phase by a constant $\pm 180°$ ($\pm\pi$ radians) at all frequencies $\left[F(\omega) \rightarrow e^{\mp j\pi} F(\omega)\right]$. From a practical standpoint, passing the signal through an invertor stage or simply reversing the input leads to a loudspeaker will accomplish this effect.

The audible effects of polarity inversion are a subject of great debate by the audio community (a comprehensive airing of the issues and an excellent tabulation of comments and references from many different sources, written from a vociferously pro standpoint, can be found in [1]). Ideally, polarity standards should be maintained in a recording and reproduction chain, so that a positive pressure (compression) at the recording microphone results in a positive pressure generated by the playback loudspeaker.

In this paper, I will not address the audibility of polarity inversion, but discuss issues pertaining to polarity measurement of band-limited systems, and specifically to polarity-like modification effects of narrow-band signal waveforms by band-limited systems and systems in general. I will show that a simple minimum-phase system can shift the phase of narrow-band signal by any arbitrary amount and produce narrow-band signal effects indistinguishable from polarity inversion.

I will describe a measurement method that evaluates the input/output narrow-band polarity-phase behavior of a system at many different frequencies. The method uses a test stimulus, that is constrained both in time and frequency, coupled with a synchronous detection scheme that allows the envelope of the test system's time response to be evaluated in amplitude, phase and delay.

An equation is presented that predicts the tone-burst phase, and hence time-constrained narrow-band polarity as a function of frequency, based on a general system's measured conventional phase and group-delay. This equation produces a more intuitive phase vs frequency curve that predicts the output phase of narrow-band transient signals, ie if the phase is ±180°, then the narrow-band input waveform will be inverted at the system's output, notwithstanding any linear-phase effects due to transport or propagation delays.

1. IMPLICATIONS OF CONVENTIONAL POLARITY DEFINITION

If polarity inversion is accomplished along with other processing (all practical systems come under this heading), in a general linear system , the inversion can be thought of as operating on the *output* of the system, rather than the input. Once the normal polarity configuration is chosen, the polarity inversion just simply inverts the time waveform of the output signal. Note that polarity evaluation, using the conventional definition mentioned in the first paragraph, makes no inference about the output of a system given a specific input. Whatever the output waveform of the system is in the normal-polarity configuration, is just simply flipped upside-down in the reversed-polarity situation. If the system's output time waveform is screwed up in the normal-polarity configuration, it will still be screwed up in the reverse polarity condition, but be upside-down!

Also note, that just simply knowing that a specific system is non-inverting tells you nothing about how the system will modify a relatively narrow-band input signal, such as a single hit on a bass kick drum. Only in the case of a flat wide-band minimum-phase electronic system, such as an amplifier or preamplifier, will knowledge of the polarity of the system give you a clue as to how the system will process a specific narrow-band input signal. More complicated systems, which may include non-minimum phase processing, such as loudspeaker systems, may modify the input signal in ways that just a simple knowledge of the polarity will not reveal.

Observe also, that because polarity reversal by definition rotates the phase of each spectral component by a constant ±180° independent of frequency, that variations of polarity, as a function of frequency, *are not allowed by definition*. The results of this conventionally-defined polarity determination result in a *single binary* (two-valued) normal-polarity or inverted-polarity judgement for *any* system, whether minimum phase, non-minimum phase, or all pass.

2. MEASUREMENT OF CONVENTIONALLY DEFINED POLARITY

Many methods have been used to measure polarity as it is conventionally defined. These include tests for tape recorders [2], magnetic reproducers [3], loudspeaker time-alignment methods [4], phono cartridges [5], and portable electro-acoustic devices for evaluating polarity of individual loudspeaker drivers [6]. These methods mostly use various wide-band asymmetrical test waveforms including triangle waves, rectangular pulses, raised cosine pulses, ramps and exponential decay pulses. Most of these methods depend on the test waveform being reproduced by the system-under-test in a somewhat faithful manner. Any out-of-the-ordinary processing by the test system, which distorts the test waveform, will complicate or invalidate the polarity determination.

To unambiguously measure the polarity of a complicated processing device, such as a loudspeaker system (which may include non-minimum-phase effects and propagation delay), requires sophisticated wide-band measurements to be made of the tested device to identify its amplitude and phase behavior [7], [8], and [9]. These measurements often need to extend over a frequency span that is considerable in excess of the bandwidth of the system being measured. In some situations, a pre-knowledge of what's being measured can significantly restrict the measured range [8].

Remember that even after accomplishing these sophisticated measurements, the polarity determination you make may not tell you what you wanted to know, ie how the system modifies a specific time-constrained narrow-band signal.

3. NARROW-BAND POLARITY MEASUREMENT METHOD

Polarity, in this context, is defined more loosely than that mentioned in the first paragraph of the introduction of this paper. It assesses the ability of a system to modify the phase of a time-limited narrow-band signal, and allows prediction of effects very similar to conventional polarity inversion. This definition of polarity directly compares the output and input of a system, but with the effects of any system or propagation delays properly accounted for. The test signal used in this measurement method is constrained both in time and frequency, as are actual music and speech signals.

What is required is a polarity determination that can be evaluated in different frequency bands. This would allow, for example, a determination of a reverse connected speaker in a multi-way system, without making individual transducer measurements. The proposed measurement method evaluates polarity phase in multiple relatively-narrow frequency bands, and does not require measurements in frequency areas that are not of interest. The measurement allows the polarity-phase wave-modification effects of systems to be evaluated at many different points across the frequency band, using a band-limited test signal.

The polarity measured in this manner can be any value in the range of ±180° (±π radians), with values near zero associated with normal polarity, and values near ±180° associated with inverted polarity. This rather strange multi-valued property of the newly defined polarity (values in the inclusive range of ±180° rather than a simple two-valued binary value) is a direct result of frequency limiting the polarity determination.

The proposed measurement method evaluates the phase polarity of the system at one-third-octave intervals across the audio band, using a Hann weighted tone-burst test signal with a one-third-octave bandwidth. The processing of the measurement system is essentially the same as that used by Shroeder [10], but with the additional capability of generating phase data along with the envelope amplitude data. The processing has been implemented on the Techron TEF System 20, a DSP based measurement system, which allows measurements to be made in real-time.

Equivalent measurements can also be made with Time Delay Spectrometry (TDS) techniques, if the phase of the complex-time response (ETC) is available and is corrected for functional form phase shift errors [11] (Note that currently, the TEF System 20 does not perform this error correction on the complex-time data).

At a specific frequency band, the tone-burst measurement process consists of the following steps:

1. Energize the system with the tone-burst signal,
2. Gather a time record of the output of the system over a specified time,
3. Evaluate the envelope of the system's output response, including amplitude and phase, using a synchronous matched in-phase/quadrature detector,
4. Determine the time of arrival of the test signal by locating the peak of the first arrival in the envelope time record (this delay includes any transport effects, such as travel through a transmission media such as air, and delays inherent in the measured system), and then
5. Evaluate the phase of the first arrival by subtracting from the measured phase, the linear phase lag equal to the systems delay (determined in step 4). Or equivalently, the phase can be directly determined by delaying the data capture of the synchronous detector by an amount equal to the time determined in step 4.

The proposed polarity-measurement method is essentially a mechanized version of the manual microphone-plugged-into-an-oscilloscope visual method, but using the proposed method's tone-burst excitation signal. In the manual method, if the scope is triggered when the burst is sent to the system under test, propagation delay simply shifts the system's output waveshape to the right across the face of the scope screen, but doesn't change its shape. The polarity determination results from visually comparing the output of the system with what went in; ie if the main-burst output is similar to the input, the polarity is normal; if the output is upside down, the polarity is inverted. Practically, the output will look neither like the input or an upside-down version of the input, this is where polarity values other than normal (0°) or inverted (±180°) come from. The output may look like a normal or inverted cosine burst, rather than the applied sine burst, which corresponds to shifts of ±90°, half-way between normal and inverted polarity!

3.1. Excitation Signal

The excitation signal is a Hann-windowed 6½-cycle sine burst, generated with the following equation:

$$f(t) = 0.5\left[1 - \cos\left(\frac{2\pi t}{6.5}\right)\right]\sin(2\pi f_0 t)$$

$$\text{for } 0 \le t \le \frac{6.5}{f_0},\ 0 \text{ otherwise} \qquad (1)$$

where

f_0 = burst center frequency, Hz

t = time, seconds.

Fig. 1 shows this burst for a 1 kHz center-frequency. The burst characteristics were chosen so that the waveform reaches a positive maximum at its center and is even symmetric about the same time point. The spectrum of the burst (not shown), is approximately one-third-octave wide at the 3-dB-down points (bandwidth ≈ 0.23 f_0), with a first sidelobe that is 32-dB down, and has skirts that roll off at 18 dB/octave for frequencies that are far from the center frequency of the burst. Fig. 2 shows bursts of various phases, at 45° increments and arranged in a circle, that represent how the burst might be modified when passed through a specific system. Note that the ±180° waveshape (burst at extreme left) is just an upside-down version of the 0° waveshape (burst at extreme right), and indicates polarity inversion. Also shown on the circle, are some suggested filled-circle graphic symbols that might be used on a response plot to graphically depict the narrow-band polarity modifications of a system (see later Figs. 14d and 15d for a possible use of these special symbols).

3.2. Detection Method

Fig. 3 shows a block diagram of the test setup including a matched synchronous detector optimized to detect the burst described in Eq. (1). The input signal is multiplied by delayed fixed-frequency (frequency equal to the center frequency of the burst) sine and cosine waves and passed through dual linear-phase low-pass filters, thus extracting the in-phase (sine channel) and quadrature-phase (cosine channel) envelopes. The output block then converts the in-phase/quadrature-phase data stream into magnitude/phase data. The detector is matched to the test burst, because the impulse response of the low-pass filters is approximately equal to the Hann-windowed waveshape $f(t) = 0.5\left[1-\cos\left(\frac{2\pi t}{6.5}\right)\right]$, used to shape the transmitted test burst.

4. PRELIMINARY THEORY

As a result of running many simulations and measurements (described in the next two main sections), the equation given shortly was found to closely predict the phase of a system's output burst at a specific frequency.

Assume the transfer function of a system is

$$H(\omega) = A(\omega)e^{j\theta(\omega)} \tag{2}$$

where

ω = frequency, rad/s, = $2\pi f$

f = frequency, Hz

$A(\omega)$ = amplitude response

$\theta(\omega)$ = phase response in radians.

Also assume the commonly defined group delay for this transfer function, which is frequency slope of the system's phase response

$$t_{group} = -d\theta(\omega) / d\omega \tag{3}$$

It was found that the following equation predicts the phase response of a system's output burst, excited by the burst of Eq. (1). This phase will henceforth be called the polarity phase.

$$\theta_{polarity}(\omega) = \theta(\omega) + \omega\ t_{group}. \tag{4a}$$

For frequency in Hz and phase in degrees, Eq. (4a) appears as:

$$\theta_{polarity}(f) = \theta(f) + 360 f\ t_{group}. \tag{4b}$$

Eq. (4) is composed of the sum of two terms: the first is just the steady-state sinusoidal phase response, and the second is a term composed of the product of the frequency and the system's group delay. The group delay was found to closely approximate the delay of the system to the tone burst inputs. The second term of Eq. (4) eliminates the effect of any propagation-delay linear-phase terms in the systems transfer function. A system composed of pure delay, just shifts the input time-domain waveform to the right, without changing its shape (or polarity). Intuitively, the polarity phase of a pure delay should be zero.

This can be illustrated as follows. Assume a system that simply delays the input by amount τ_d (all linear-phase systems have this form of phase response):

$$H(\omega) = e^{-j\omega\tau_d} = e^{j-\omega\tau_d} = e^{j\theta(\omega)}. \tag{5}$$

The group delay of this system is, of course, just τ_d. The polarity phase Eq. (4) then yields

$$\begin{aligned}\theta_{polarity}(\omega) &= \theta(\omega) + \omega\ t_{group} \\ &= -\omega\tau_d + \omega\tau_d \\ &= 0\end{aligned}$$

as expected.

In the next two sections, application of Eq. (4) and the results of tone-burst measurements for various filter functions and experimental loudspeaker response measurements, are illustrated.

5. APPLICATION

The polarity-phase response function of Eq. (4), and a computer-simulated implementation of the tone-burst polarity measurement setup of Fig. 3, was used to evaluate several different types of filters. These included four different types of minimum-phase filters: shelf, low-pass, high-pass, and band-pass; and two types of all-pass filters: first-order and second-order. The range of filters simulated was not exhaustive and only included a few representative types and orders. Data displayed for each type of filter included: magnitude response, phase, group delay, and polarity phase.

The simulations were run on a Macintosh II computer using the excellent simulation program called "Extend" (Imagine That, Inc., 151 Bernal Road, Suite 5, San Jose, CA 95119-1306 USA, (408) 365-0305). The block diagram, shown in Fig. 3, was extracted from the Extend simulation for these experiments.

5.1. Introductory Simulation

A simulation was accomplished on a representative system composed of a 40-Hz fourth-order Butterworth high-pass filter in cascade with a pure delay of 0.1 second. This system could represent the output of a vented-box low-frequency speaker system with an acoustic propagation delay. A single simulation was done at 80 Hz, which is one octave above the system's 40-Hz 3-dB-down cutoff frequency. The output of this simulation is shown in Fig. 4. A simulation time of 0.25 s was used with 1000 simulation steps from start to finish.

Fig. 4a shows the tone burst applied to the input of the system. The burst lasts for 81.25 ms (= 6.5/80), centered at 40.625 ms. Fig. 4b shows the output of the envelope detector, connected directly to the test source. Both magnitude (solid line) and phase (grey line) are shown as a function of time. The envelope magnitude reaches a maximum at 81.00 ms, where the phase is 0°. The output of the envelope detector lags the input burst due to the delay of the low-pass smoothing filters.

Fig. 4c illustrates the output of the system. It appears to be shifted to the right by about 100 ms and inverted. Fig. 4d indicates the detector output when connected to the system output. An envelope maximum occurs at 184.25 ms, indicating a system delay of 103.25 ms (= 184.25 - 81.00), where the phase is +174.9°. One hundred miliiseconds of the delay is due to the modeled propagation delay, and 3.25 ms is due to the delay of the high-pass filter. Fig. 4e shows a delayed version of the input signal, delayed by an amount which matches it with the system's output. Fig. 4f shows an expanded version of the system's output superimposed on the delayed burst of Fig. 4e. This clearly shows that the output of the system is inverted with respect to the input, and is effectively polarity reversed. Later, a general analysis of the fourth-order Butterworth high-pass filter will be accomplished (Sec. 5.4), which will show why this filter inverts at the relatively high frequency of an octave above its cutoff.

5.2. Shelf Filter

The polarity-phase response function of Eq. (4), and a computer-simulated implementation of the tone-burst polarity measurement setup of Fig. 3, was used to evaluate the first-order low-frequency shelf function:

$$H(s) = \frac{s + 1/\sqrt{10}}{s + \sqrt{10}} \approx \frac{s + 0.3162}{s + 3.162} \qquad (6)$$

where

s = complex variable = $j\omega = j2\pi f$

f = frequency, Hz.

This function provides a 20 dB shelf at low-frequencies ($\omega << 1$), and unity gain at high frequencies ($\omega >> 1$). This specific function was chosen because it exhibits negative group below $\omega = 1$, and is discussed by Heyser [12].

Fig. 5 depicts the results of computer evaluation of the shelf function of Eq. (6), and the results of the simulated tone-burst measurements. Figs. 5a through 5d. show respectively: the magnitude vs frequency, phase vs frequency, group delay vs frequency, and polarity phase vs frequency evaluated using Eq. (4). Also in Figs. 5c and 5d are the tone-burst test results shown with boxed data points. These and the following graphs have been normalized so that the critical frequency of the filter occurs at 1 Hz, and have been plotted over the range of 0.1 to 10 Hz, using a log frequency scale.

Based on the results of the computer-simulated implementation of the tone-burst polarity measurement setup of Fig. 3 (boxed data points in Fig. 5c), it appears that the group delay is a good predictor of the arrival time of the tone burst. The agreement is good even in the range where the group delay is negative. In this range, the tone-burst arrival time (peak of the envelope) actually preceded the envelope peak when the detector was hooked directly to the burst generator!

This does not mean that the system is non-causal, however, because the burst waveform was slightly compacted on its left edge thus moving the peak slightly to the left on the time axis. In the range $\omega < 1$, the absolute value of group delay is small in proportion to the total burst length. For example, at $f = 0.5$ Hz the group delay is 0.30 secs, which is only 2.3% (=0.3 x 0.5 / 6.5 x 100%) of the total burst length (13 s).

In Fig. 5d, the polarity phase is shown evaluated using Eq. (4). In general, where the group delay is negative, the conventional phase of Fig. 5b is pulled down, and where the group delay is positive, the conventional phase is raised up. Also note in Fig. 5d, the close correspondence between the tone-burst evaluated polarity phase and the computed polarity phase, using Eq. (4).

5.3. Low-Pass Filters

The polarity-phase responses of the following first- and second-order Butterworth low-pass filters were evaluated using Eq.(4):

$$H_{LP1st}(s) = \frac{1}{s + 1}, \quad \text{and} \qquad (7)$$

$$H_{LP2nd}(s) = \frac{1}{s^2 + \sqrt{2}s + 1}. \qquad (8)$$

These results are shown in Figs. 6 and 7 along with magnitude, phase, and group delay responses. Tone-burst evaluated polarity-phase data is also shown in Fig. 7d for the 2nd-order low-pass filter; note the close agreement. A comparison of the polarity-phase curves of both filters (Figs. 6d and 7d) with the conventional phase curves (Figs. 6b and 7b), reveals that in general, the polarity-phase curve is shifted up and to the right, making the polarity phase unsymmetrical with respect to the 1-Hz corner frequency of the filters.

Note surprisingly, that for the 2nd-order filter (and to a lesser extent for the 1st-order filter), that even though the steady-state sinusoidal phase decreases to 90° at its cutoff frequency, the polarity phase stays essentially constant at 0° up to the cutoff! Note also, that in general, the polarity-phase curve predicts an improvement in the pass band of the low-pass filters, ie the filter preserves 0° tone-burst phase all the way up to cutoff.

5.4. High-Pass Filters

The following Butterworth high-pass filters of first, second, and fourth order were evaluated for polarity response using Eq. (4):

$$H_{HP1st}(s) = \frac{s}{s+1}, \tag{9}$$

$$H_{HP2nd}(s) = \frac{s^2}{s^2+\sqrt{2}s+1}, \text{ and} \tag{10}$$

$$H_{HP4th}(s) = \frac{s^2}{s^2+0.7653s+1} \bullet \frac{s^2}{s^2+1.84776s+1}$$

$$= \frac{s^4}{s^4+2.613s^3+3.414s^2+2.613s+1}. \tag{11}$$

Figs. 8 to 10 depict the responses for these three high-pass filters. As before, filter magnitude, phase, group delay, and polarity-phase curves are displayed. Note that, as was the case with the low-pass filters, the polarity phase (Figs. 8d, 9d, and 10d) is shifted up and to the right, as compared to the steady-state phase (Figs. 8b, 9b, and 10b). The shift up of polarity phase of the 2nd-order filter (Fig. 8d), actually triggers an additional wrap in phase at about 0.88 times its cutoff (compare Fig. 9d with 9b)!.

In general, the phase-polarity curve predicts that the poor behavior (in modifying tone-burst phase) of the high-pass filters below cutoff, is actually moved farther up into the filter's pass band. This is in contrast with the low-pass filters, where the polarity phase predicted an improvement in pass-band behavior. Note, that the second-order high-pass filter (Fig. 9d) acts as a polarity invertor for all frequencies near cutoff and below! Also note, that the fourth-order high-pass filter (Fig. 10d), exhibits polarity inversion in the pass-band approximately an octave above cutoff (refer back to the introductory simulation in section 5.1 for waveshapes at this frequency)! Observe, that the group-delay peak of the fourth-order filter at 0.9 Hz (Fig. 10c), shows up in the polarity phase (Fig. 10d) at the same frequency.

5.5. Band-Pass Filter

A Butterworth second-order band-pass filter was evaluated, with the following transfer function:

$$H_{BP2nd}(s) = \frac{s}{s^2 + \sqrt{2}s + 1}. \qquad (12)$$

The response curves for this filter are shown in Fig. 11. The magnitude response of the filter rolls off symmetrically, on either side of its center frequency, at 6 db per octave (Fig. 11a). The steady-state phase smoothly changes from +90° at low frequencies, to 0° at the center frequency, and to -90° at high frequencies (Fig. 11b). The polarity phase (Fig. 11d), in contrast, stays at +90° all the way up to the filter's center frequency, and then smoothly decreases to 0° at higher frequencies. [Side note: When I first experimented with the computer-simulated tone-burst detection scheme of Fig. 3, one of the first tests, I accomplished, was evaluating a second-order bandpass filter at its center frequency. The resulting 90° phase advance was a bafflement, because my intuition predicted that the phase should be zero, due to the symmetries of the filter.]

5.6. All-Pass Filters

Both first- and second-order all-pass filters (with Butterworth polynomials) were analyzed in this section:

$$H_{AP1st}(s) = -\frac{s-1}{s+1}, \qquad \text{and} \qquad (13)$$

$$H_{AP2nd}(s) = \frac{s^2 - \sqrt{2}s + 1}{s^2 + \sqrt{2}s + 1}. \qquad (14)$$

The results for these filters are shown in Figs. 12 and 13. As before, the polarity-phase curves (Figs. 12d and 13d) are shifted up and to the right, as compared to the steady-state phase curves (Figs. 12b and 13b). As was the case for the low-pass filters (Figs. 6 and 7), the polar phase predicts that the 0° low-frequency polarity phase of these filters is extended up farther in frequency. The polarity phase of the second-order filter (Fig. 13d), essentially stays at 0° all the way up to the center frequency of the filter, where the steady-state phase is 180°! For the second-order filter, the polarity phase predicts that a phase inversion will occur one octave above the center frequency of the filter.

6. EXPERIMENTAL MEASUREMENTS

Two different types of tower-style domestic all-direct-radiator multi-way loudspeaker systems were selected for evaluation.

The first is moderate-to-high-priced three-way vented-box system composed of a 10-in. cone woofer, 6-in. cone midrange, and a 1-in. dome tweeter. The lower crossover of this system is placed low at 250 Hz, using an 18 dB/octave Butterworth design, with the woofer wired in reverse polarity. The upper crossover is an all-pass 24-dB/octave Linkwitz-Riley design, located at 2.2 kHz.

The second is very-expensive high-end five-way closed-box system designed for complete time and phase coherence. The system uses three 8-in. cone woofers, 5-in. cone midrange, 2-in. dome upper-midrange, and a 1-in. dome tweeter. The crossover frequencies are at 50 Hz, 400 Hz, 1 kHz, and 3 kHz. This system has a large extremely complex crossover which includes all-pass delay filters to align the drivers for overall linear-phase response.

Figs. 14 and 15 show the measurement results for each of these two loudspeaker systems. As before, magnitude, phase, group delay, and polarity-phase responses are illustrated. Eq. (4) was used to compute the polarity phases for each system (Figs. 14d and 15d). In addition, a complete set of one-third-octave tone-burst measurements were made on the first system, using the TEF System 20 measurement box. These measurements are shown on the polarity-phase graph (Fig. 14d), with boxed data points.

The measurement data for the first system was gathered outside, using the ground plane technique, which provided valid data down to 20 Hz. The levels have been adjusted to yield a standard sensitivity 2.83 Vrms / 1 m curve. The second system was measured in my listening room, at a distance of 3 m, with the test microphone at a height of 36", which is the designed on-axis listening axis of the system. The time resolution of the test sweep was set to 2 ms, which allows only the direct sound of the system to be measured. Only response data above 100 Hz was gathered. Because of the narrow time resolution, the response data below 500 Hz is questionable. The receive delay of the measurement was set to equal the propagation delay of the speaker to microphone.

The phase and group delay data for the first system (Figs. 14b and 14c), is quite similar overall to many other domestic speaker systems. Most of these systems have the acoustic centers of their midrange and woofer, located behind the tweeter. If phase measurements are made with the analyzer referenced to the tweeters arrival time, the resultant phase curve is flat in the tweeters range and then typically rises with decreasing frequency below the upper crossover (Fig. 14b) [13]. The group delay of the first system (Fig. 14c) is flat in the tweeters range, and then rises with decreasing frequency, which reflects the rearward acoustic positions of the midrange/woofer and the system's crossover design.

The first systems polarity phase is shown in Fig. 14d. The agreement between the tone burst measurements (boxed data points) and the computed polarity-phase curve is quite good. The tone-burst measurement data at 20 Hz, 25 Hz, 400 Hz, and 5 kHz appear to be renegades, but in fact are not, because of phase wrapping. If the phase data were plotted un-wrapped, the agreement would visually be quite close.

The first-system's polarity data (Fig. 14d), exhibits two major phase wraps, one near 250 Hz due to the lower crossover, and one at 4 kHz, about 1 octave above the upper crossover. Because the polarity-phase data for this system is spread out over the whole $\pm 180^\circ$ phase range, it will not faithfully preserve the phase or polarity of any signal passed through it. Above 8 kHz, the polarity phase of the system actually stays within 100° to 130°, which is neither in or out of phase.

The measurement data for the second system is shown in Fig. 15. The phase data in Fig. 15b, clearly shows the linear phase nature of the system. Between 100 Hz and 20 kHz, the phase only varies about $\pm 20^\circ$ around the 0° line. The remaining undulations in the phase curve are presumable due to minimum phase variations corresponding to peaks and dips in the magnitude curve (Fig. 15a). The group delay and polarity-phase curves (Figs. 15c and d) are equally well behaved. Because of the small variations in the polarity-phase response, this system is expected to preserve well the phase or polarity of signals passed through it. Note however, that this is true only at the designed listening axis, at other points higher or lower in the vertical plane, the linear-phase nature of the system is degraded.

Even though the polarity-phase results of the two systems differed by a considerable amount, they both ranked quite highly in listening tests.

7. CONCLUSIONS

Conventionally-defined polarity inversion flips the time waveform of a system upside-down. Frequency wise, polarity inversion rotates the phase of each spectral component of a signal by $\pm 180°$ ($\pm\pi$ radians) at all frequencies. By definition, polarity assessment results in a single binary (two-valued) normal-polarity or inverted-polarity judgement for any system. Variations of polarity with frequency, are not allowed by definition.

Polarity tells you nothing about the input/output behavior of a system. The polarity operator, applied to a linear system, can be thought of as acting on the output of the system. Once the normal polarity configuration is chosen, the polarity inversion just simply inverts the time waveform of the output signal. Whatever the output of the system is in the normal-polarity configuration, is just simply flipped upside-down in the reversed polarity-situation. If the system's output time waveform is distorted in the normal-polarity configuration, it will still be as distorted in the reverse polarity condition, but be upside-down.

A new definition of polarity was proposed that bases the polarity assessment on the response of a system to a time-limited narrow-band test signal. The proposed narrow-band polarity-phase assessment allows variations with frequency, and permits values over the complete range of $\pm 180°$. Polarity phase values covering the complete range of $\pm 180°$, are a direct result of limiting the frequency range of the proposed polarity-phase assessment. Knowledge of the polarity phase directly yields information about the output of a system, given a specific time-constrained narrow-band input signal. In a specific frequency band, values of polarity phase near 0° denotes a normal polarity situation, and values near 180° signify an inverted polarity situation. Other phase values denote situations that are between normal and inverted polarity.

A measurement technique has been presented, that allows the proposed polarity-phase behavior of a system to be measured at many different frequencies. The technique is based on the use of a Hann-windowed tone burst, coupled with a matched synchronous detector, which yields the envelope amplitude and phase of the measured system's output. The tone-burst phase, at the peak of the first arrival of the system's output, yields the desired polarity-phase value.

An equation was presented, that allows the polarity phase to be computed from the conventional steady-state sinusoidal phase and group delay responses of a system. The polarity-phase equation is composed of the sum of two terms: the first is just the conventional phase and the second is composed of the product of frequency times the group delay of the system. The polarity-phase equation essentially removes any linear-phase components of a systems response, and directly yields polarity-like phase response data vs frequency, that predicts how a specific narrow-band input signal will be modified at the output. The polarity-phase response curve is more intuitive than a standard phase response, because it in effect tells you whether a system inverts or not (or any where in between) in any particular frequency band.

An analysis was made of several different types of minimum and non-minimum-phase filters. For most filters with positive group delay, this study revealed that phase values were increased in level and effectively shifted higher in frequency, when the polarity-phase data was compared with the conventional steady-state sinusoidal phase data. In general, the polarity-phase performance of low-pass filters was significantly better that the performance of high-pass filters. The polarity phase of the analyzed low-pass filters is well behaved (ie near 0°) right up to cutoff. In contrast, for higher-order high-pass filters, polarity inversions are exhibited in the pass band at frequencies significantly higher than the filter's cutoff.

8. ACKNOWLEDGEMENT

I am indebted to Kieth Jebelian for programming the TEF20 measurement system to do tone-burst tests according to the proposed method. Much appreciation also goes to Brian Flinn, who did the Macintosh high-level programing to control the TEF20. Thanks also to Techron and *Audio* Magazine for allowing me the time and use of equipment to accomplish this research.

9. REFERENCES

[1] R. C. Johnsen, "The Wood Effect," Harvard University Press, Cambridge, MA (1988) (Book available from the Modern Audio Association, 23 Stillings St., Boston, MA 02210, Phone: (617) 423-4590).

[2] J. Vanderkooy and S. P. Lipshitz, "Polarity and Phase Standards for Analog Tape Recorders," presented at the 69th Convention of the Audio Engineering Society, Los Angeles, 1981 May 12-15, preprint no. 1795.

[3] P. Butt, "A Proposed Method for Uniform Determination of Polarity of magnetic Reproducers," presented at the 66th Convention of the Audio Engineering Society, Los Angeles, 1980 May 6-9, preprint no. 1651.

[4] E. M. Long, "A Time-align Technique for Loudspeaker System Design," presented at the 54th Convention of the Audio Engineering Society, Los Angeles, 1976 May 4-7, preprint no. 1651.

[5] T. Muraoka, H. Onoye, and A. Takayanagi, "Measurement of Phonograph Cartridges by the Pulse Train Method," J. Audio Eng. Soc., vol. 22, no. 7, p. 502 (1974 Sept.).

[6] Dynaudio USA, Inc., "Phase Test Equipment," A small portable test box for checking polarity, that generates a 5 pulse per second (each pulse is an exponential decay formed by discharging a capacitor through a resistor) pulse train, and has a built in microphone and processing to drive red/green LED indicators for indicating normal or reverse polarity.

[7] R. Heyser,"Determining the Acoustic Position for Proper Phase Response of Transducers," J. Audio Eng. Soc., vol. 32, no. 1/2, pp. 23-25 (1984 Jan./Feb.).

[8] S. Lipshitz and J. Vanderkooy, "Comments on "Determining the Acoustic Position for Proper Phase Response of Transducers"," J. Audio Eng. Soc., vol. 33, no. 6, pp. 463-465 (1985 June).

[9] R. Heyser, Authors Reply to "Comments on "Determining the Acoustic Position for Proper Phase Response of Transducers"," J. Audio Eng. Soc., vol. 33, no. 6, pp. 465-466 (1985 June).

[10] B. Atal, M. Schroeder, G. Sessler, and J. West, "Evaluation of Acoustic Properties of Enclosures by Means of Digital Computers," J. Acous. Soc. Am., vol. 40, no. 2, pp. 428-433 (1966 March).

[11] P. D'Antonio, J. Konnert, "Complex Time Response Measurements Using Time-Delay Spectrometry," J. Audio Eng. Soc., vol. 37, no. 9, pp. 674-690 (1989 Sept.).

[12] R. Heyser,"Loudspeaker Phase Characteristics and Time Delay Distortion: Part 2," J. Audio Eng. Soc., vol. 22, no. 7, pp. 130-137 (1969 April).

[13] D. B. Keele, Jr., Various loudspeaker reviews published in *Audio* magazine, see issues 1988 Feb.; 1989 Sept.; 1990 July, Aug., Nov., Dec.; 1991 Jan., Aug.

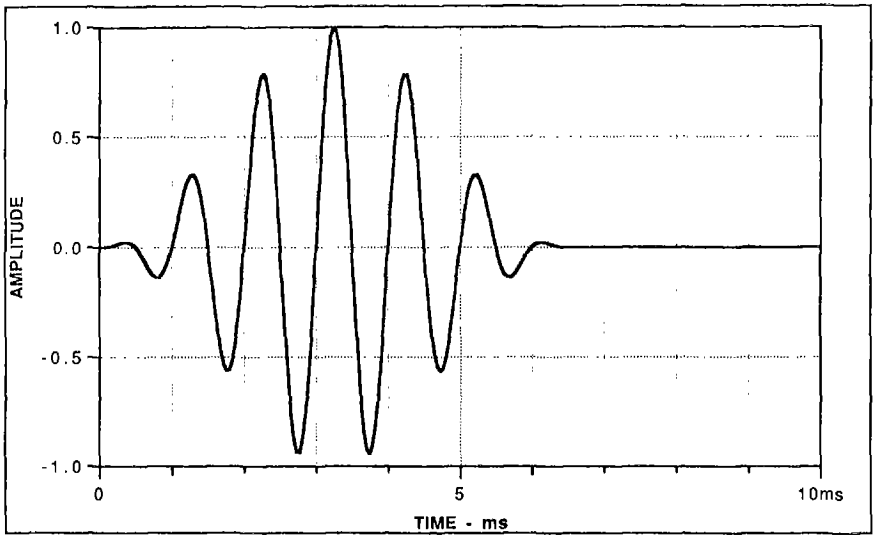

Fig. 1. Tone-burst test signal used to evaluate time-constrained narrow-band phase. The signal is a Hann-windowed 6 1/2-cycle sinewave burst, whose spectrum is approximately one-third-octave wide at the 3-dB down points. The burst is shown for a 1 kHz center frequency.

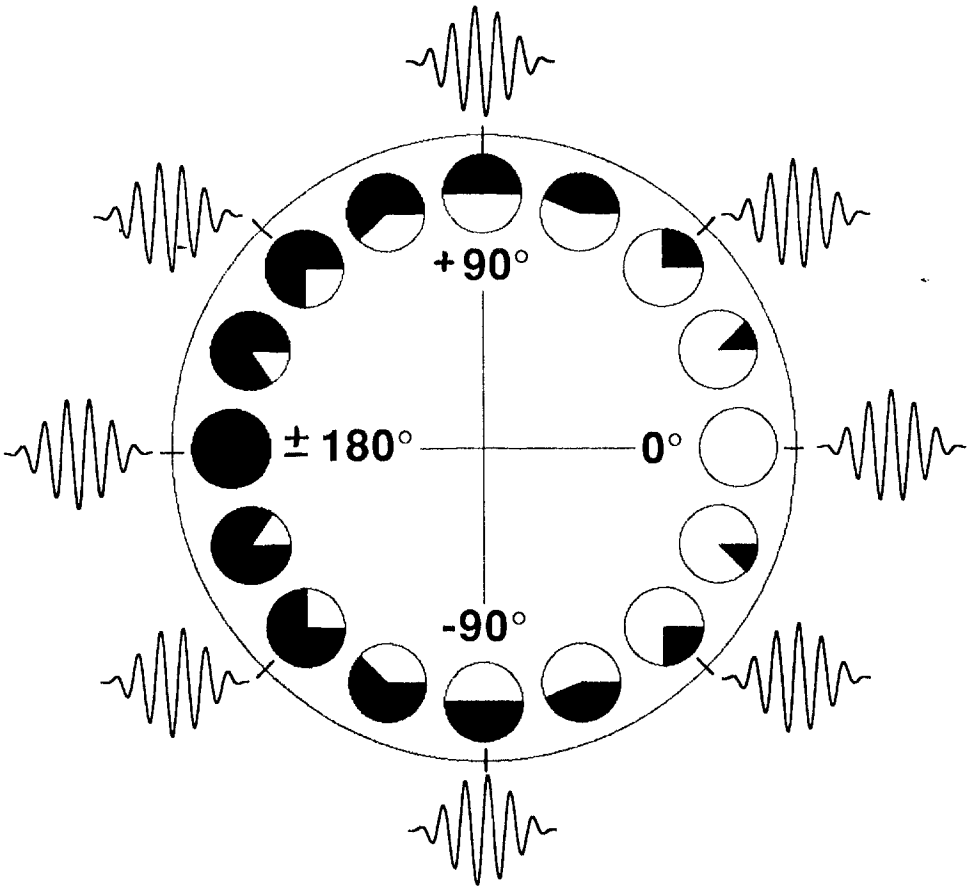

Fig. 2. Polarity-phase circle illustrating various burst phases in the range of ±180°. Also shown are suggested filled-circle graphic symbols that might be used with response curves to depict polarity phase at different frequencies. An empty circle indicates 0° normal polarity (far right) and a completely black-filled circle depicts 180° inverted polarity (far left). In between phase values are shown with various proportions of fill, with the fill direction indicating the plus/minus phase value.

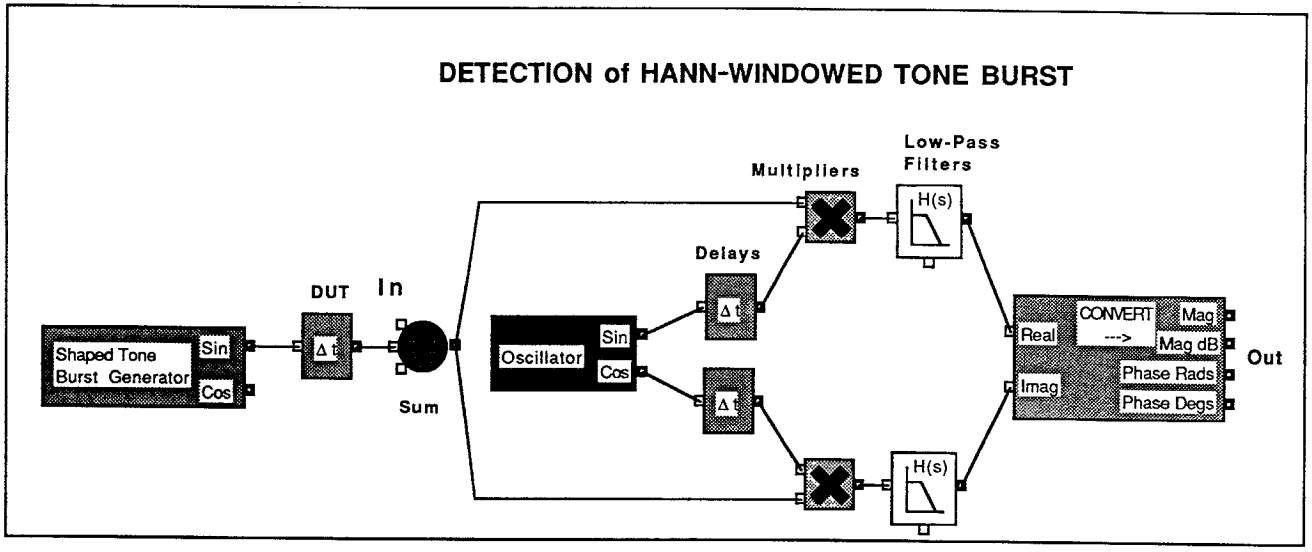

Fig. 3. Block diagram of matched synchronous detector, optimized to detect the burst shown in Fig. 1. The envelope output of the detector allows the amplitude and phase of a system's tone-burst time response to be determined.

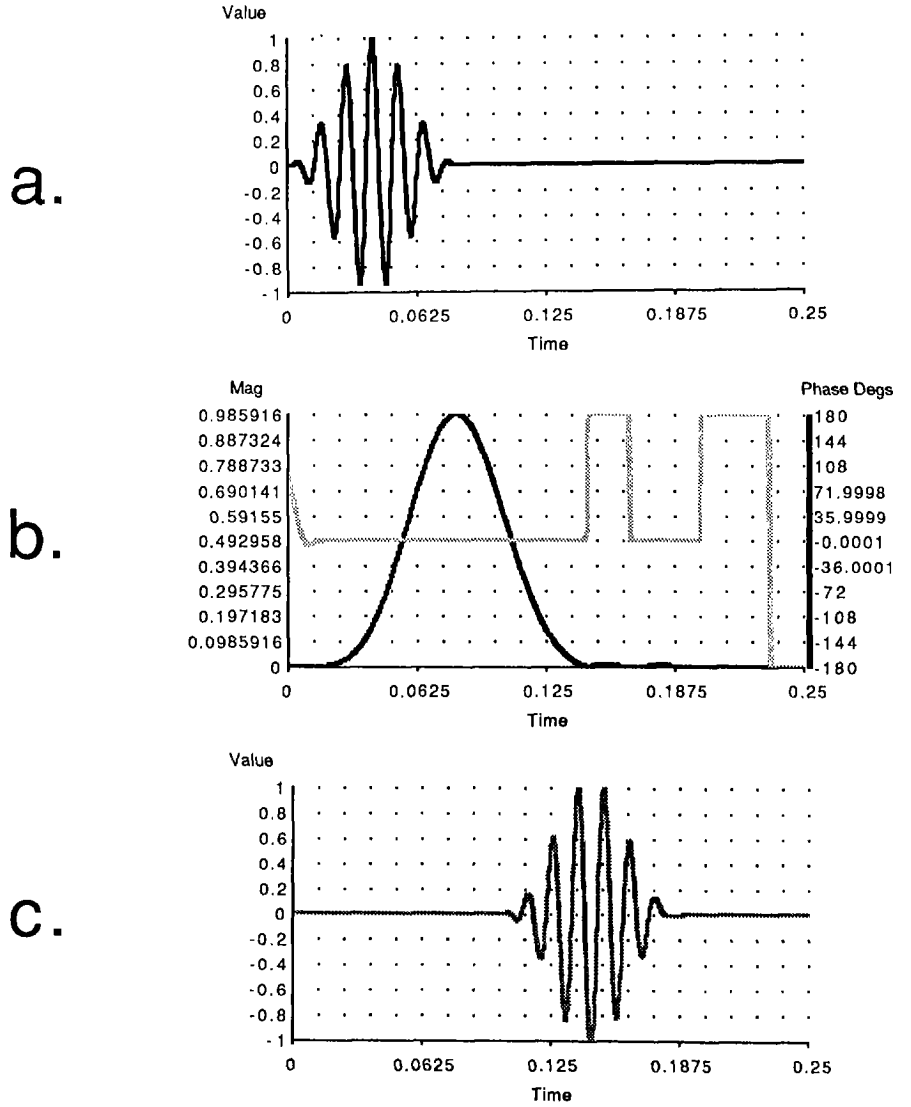

Fig. 4. Series of time response graphs, for the detector system of Fig. 3, illustrating the 80-Hz tone-burst response of a system composed of a 40-Hz 4th-order Butterworth high-pass filter cascaded with a 0.1 second delay element. (a) Amplitude vs time of tone-burst test signal. (b) Magnitude (solid line) and phase (grey line) time responses of envelope detector when connected directly to tone-burst test signal. Note 0° phase at envelope peak. (c) Amplitude vs time of output of system. Note that the output is an inverted version of the input. (d) Magnitude (solid line) and phase (grey line) time responses of envelope detector when connected to output of system. Note +180° phase at envelope peak. (e) Amplitude vs time of tone-burst test signal that is delayed by 103.25 ms. This delay matches the measured delay of the tested system. (f) An expanded amplitude vs time response of the bursts of (c) and (e), plotted on the same graph to illustrate their 180° inverted relationship.

d.

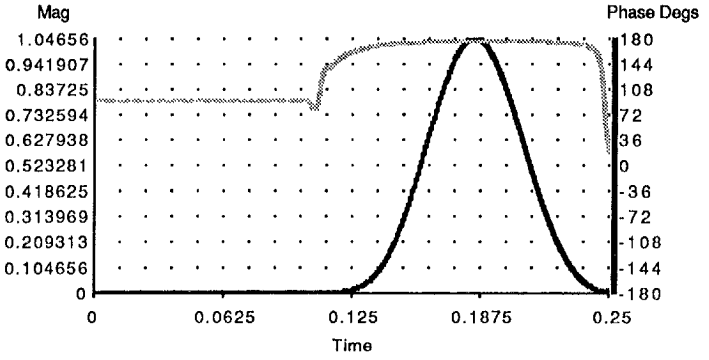

e.

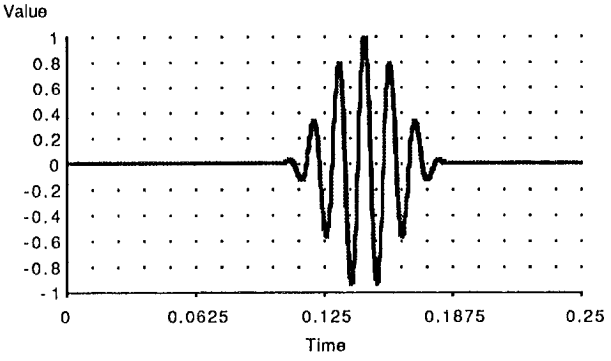

f.

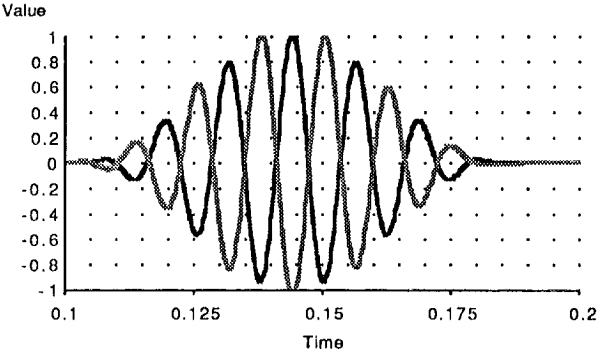

Fig. 4. Continued

a.

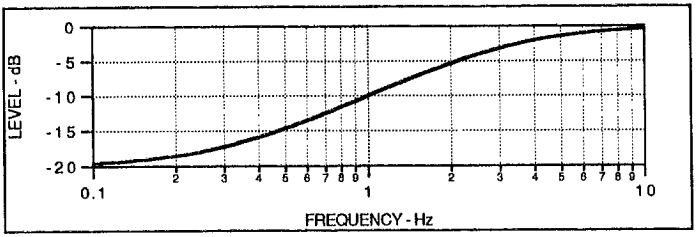

b.

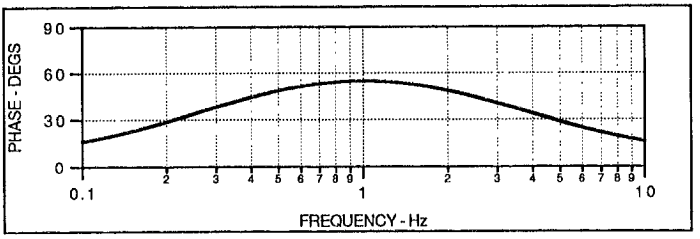

c.

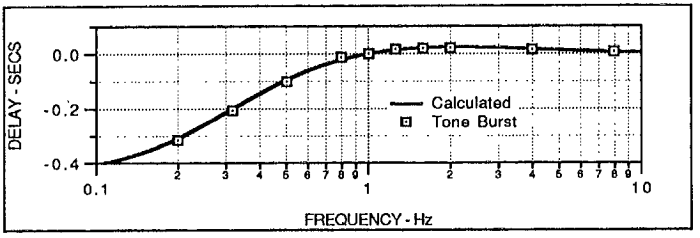

d.

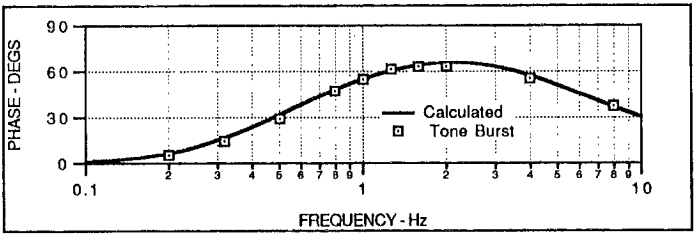

Fig. 5. Series of graphs illustrating various responses of the first-order low-frequency shelf function of Eq. (6), plotted over the range of 0.1 to 10 Hz. (a) Magnitude vs frequency. (b) Phase vs frequency. (c) Group delay vs frequency. (d) Polarity phase vs frequency. Curves (c) and (d) contain both calculated and tone-burst measured data. Note the close agreement between the two. The calculated polarity-phase data was derived from the phase (b) and group delay (c) using Eq. (4).

a.

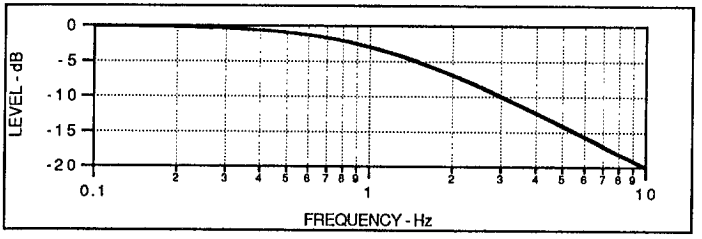

b.

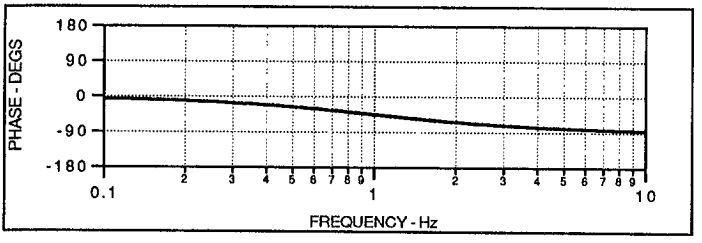

c.

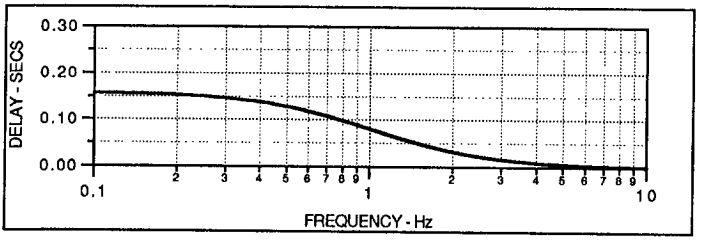

d.

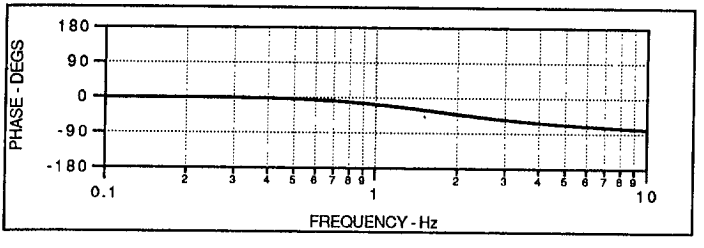

Fig. 6. Response curves for the 1-Hz first-order low-pass filter of Eq. (7), plotted over the range of 0.1 to 10 Hz. (a) Magnitude vs frequency. (b) Phase vs frequency. (c) Group delay vs frequency. (d) Polarity phase vs frequency calculated using Eq. (4).

a.

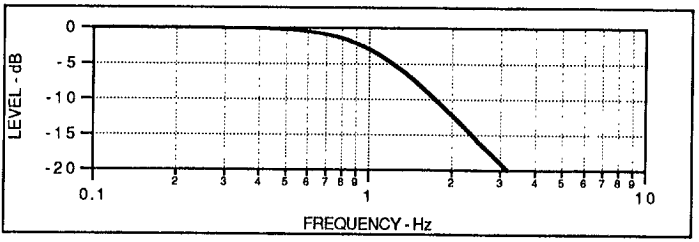

b.

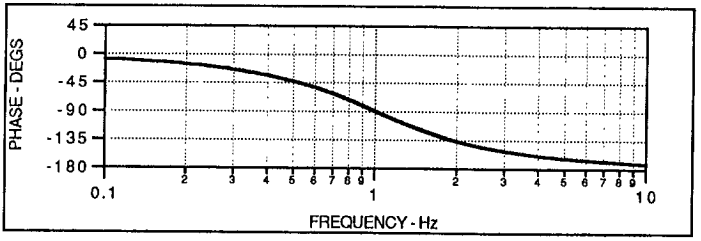

c.

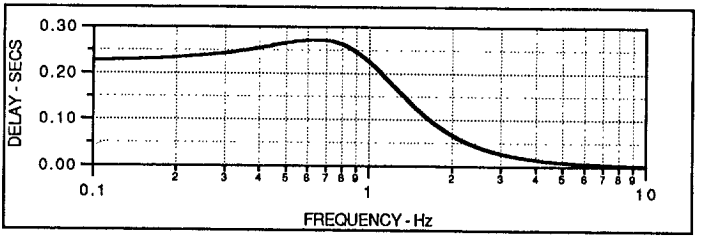

d.

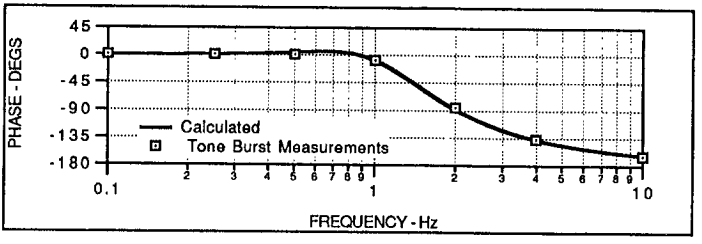

Fig. 7. Response curves for the 1-Hz second-order low-pass filter of Eq. (8), plotted over the range of 0.1 to 10 Hz. (a) Magnitude vs frequency. (b) Phase vs frequency. (c) Group delay vs frequency. (d) Polarity phase vs frequency. Graph (d) contains both calculated and tone-burst measured data, which are in close agreement. Note the flatness of the polarity phase up to the filters 1-Hz cutoff frequency. This is despite a -90° value in the conventional phase at cutoff.

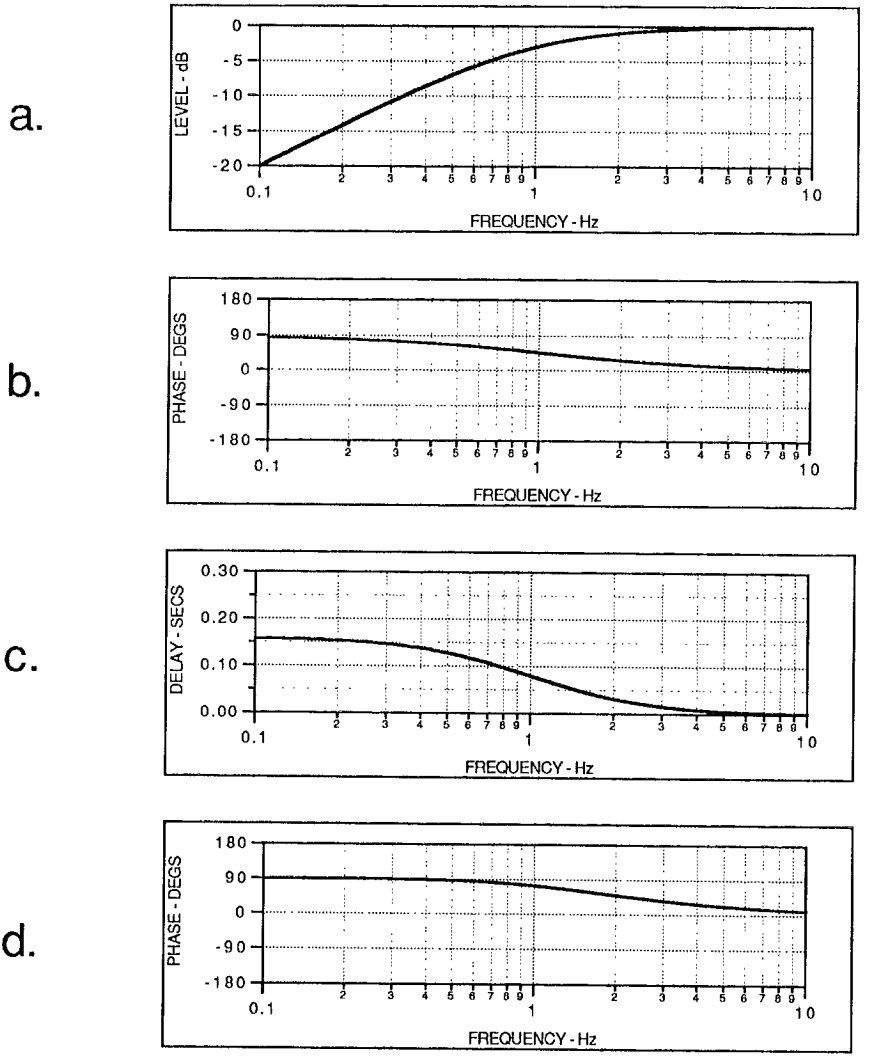

Fig. 8. Response curves for the 1-Hz first-order high-pass filter of Eq. (9), plotted over the range of 0.1 to 10 Hz. (a) Magnitude vs frequency. (b) Phase vs frequency. (c) Group delay vs frequency. (d) Polarity phase vs frequency calculated using Eq. (4).

a.

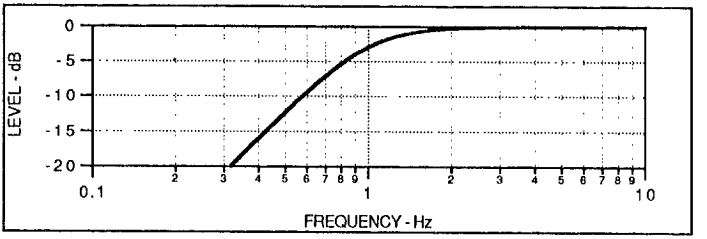

b.

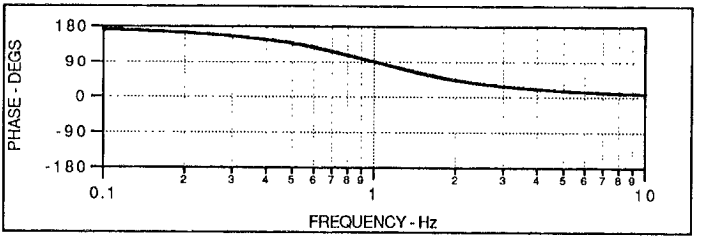

c.

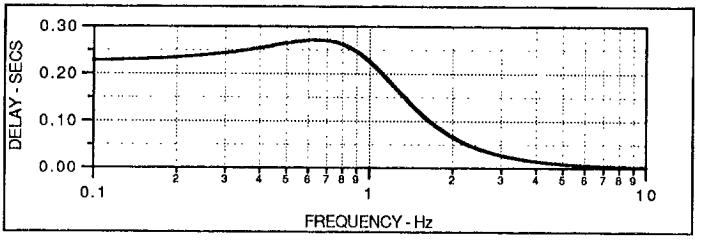

d.

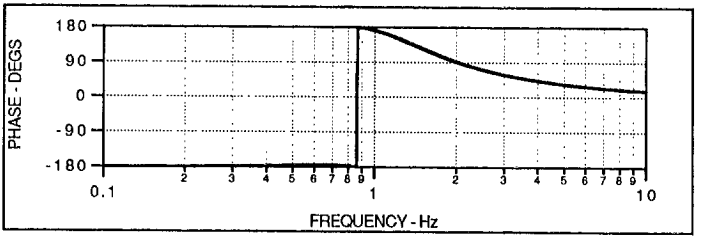

Fig. 9. Response curves for the 1-Hz second-order high-pass filter of Eq. (10), plotted over the range of 0.1 to 10 Hz. (a) Magnitude vs frequency. (b) Phase vs frequency. (c) Group delay vs frequency. (d) Polarity phase vs frequency calculated using Eq. (4). Note the 180° inverting polarity phase at cutoff and below.

a.

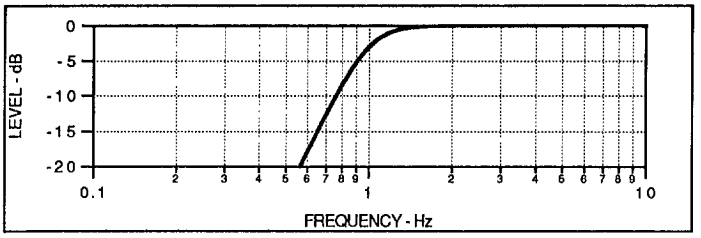

b.

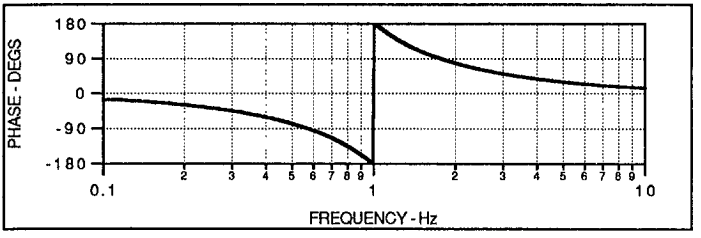

c.

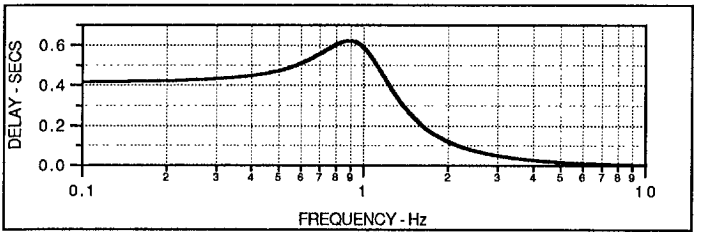

d.

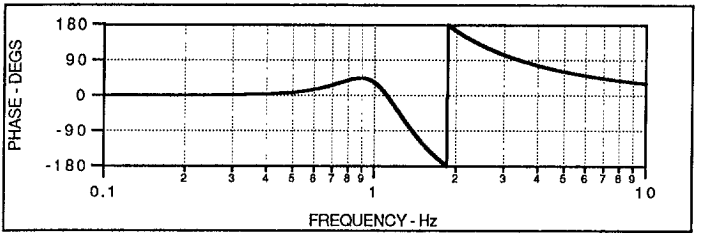

Fig. 10. Response curves for the 1-Hz fourth-order high-pass filter of Eq. (11), plotted over the range of 0.1 to 10 Hz. (a) Magnitude vs frequency. (b) Phase vs frequency. (c) Group delay vs frequency. (d) Polarity phase vs frequency calculated using Eq. (4). Note that the filter exhibits inverting 180° polarity phase at an octave above cutoff.

a.

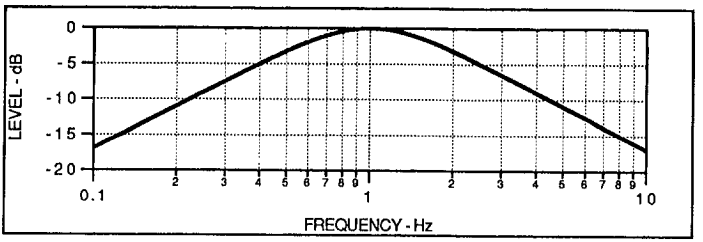

b.

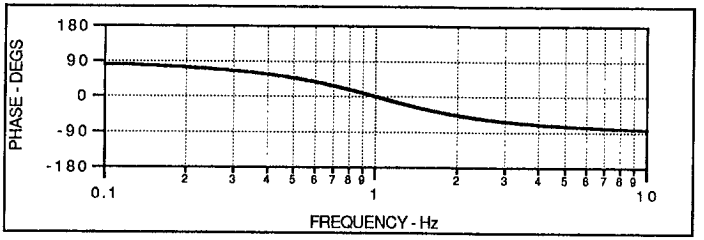

c.

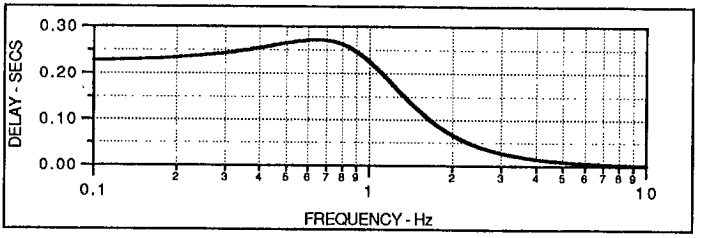

d.

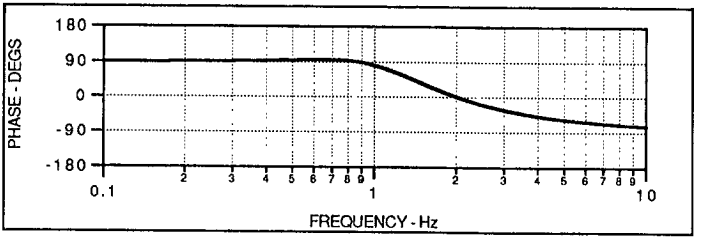

Fig. 11. Response curves for the 1-Hz second-order band-pass filter of Eq. (12), plotted over the range of 0.1 to 10 Hz. (a) Magnitude vs frequency. (b) Phase vs frequency. (c) Group delay vs frequency. (d) Polarity phase vs frequency calculated using Eq. (4). Note that the polarity phase at the center of the bandpass is about 90°, rather than the 0° value that might be expected from observing the traditional phase response (b).

a.

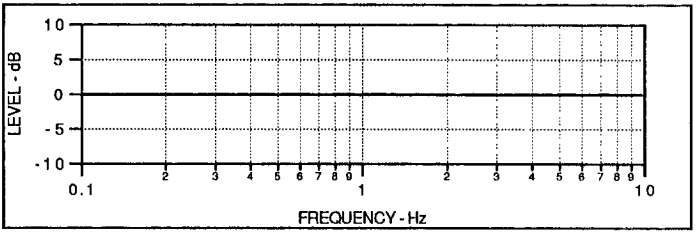

b.

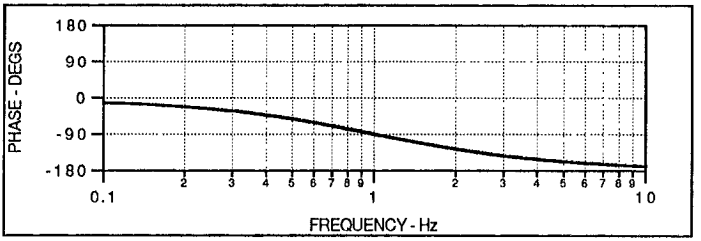

c.

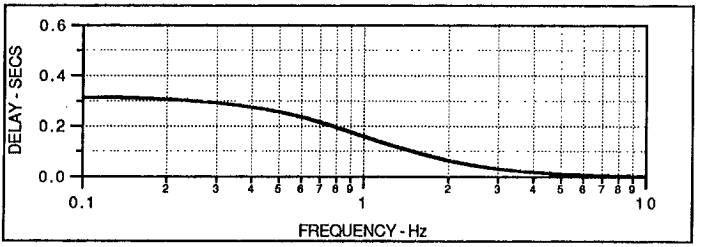

d.

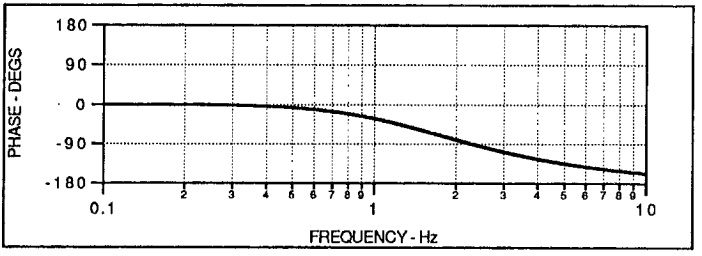

Fig. 12. Response curves for the first-order all-pass filter of Eq. (13), plotted over the range of 0.1 to 10 Hz. (a) Magnitude vs frequency. (b) Phase vs frequency. (c) Group delay vs frequency. (d) Polarity phase vs frequency calculated using Eq. (4).

a.

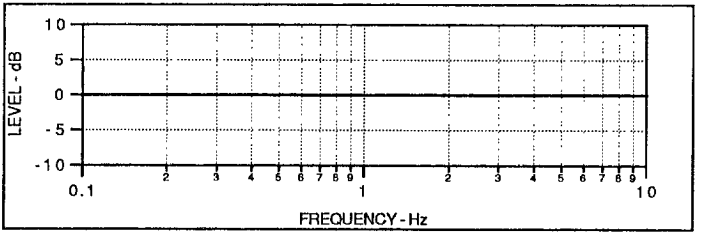

b.

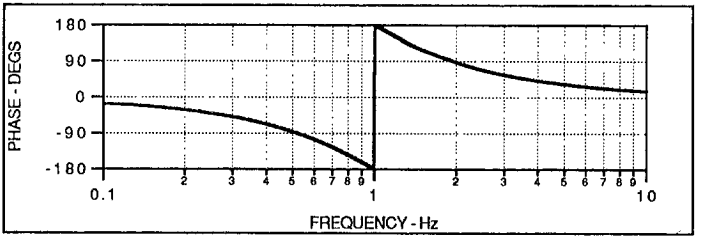

c.

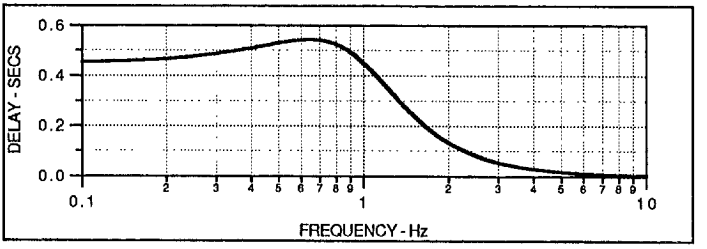

d.

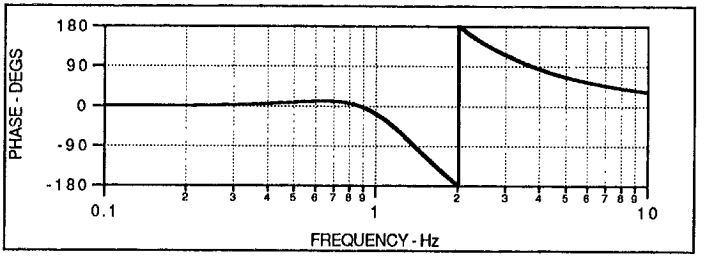

Fig. 13. Response curves for the second-order all-pass filter of Eq. (14), plotted over the range of 0.1 to 10 Hz. (a) Magnitude vs frequency. (b) Phase vs frequency. (c) Group delay vs frequency. (d) Polarity phase vs frequency calculated using Eq. (4). Surprisingly, the polarity phase is quite flat all the way to the filter's 1-Hz turnover frequency. Analysis of the conventional phase (b) would lead one to believe that the filter should invert at the turnover frequency. The polarity-phase inversion point actually occurs at an octave above the filter's turnover frequency.

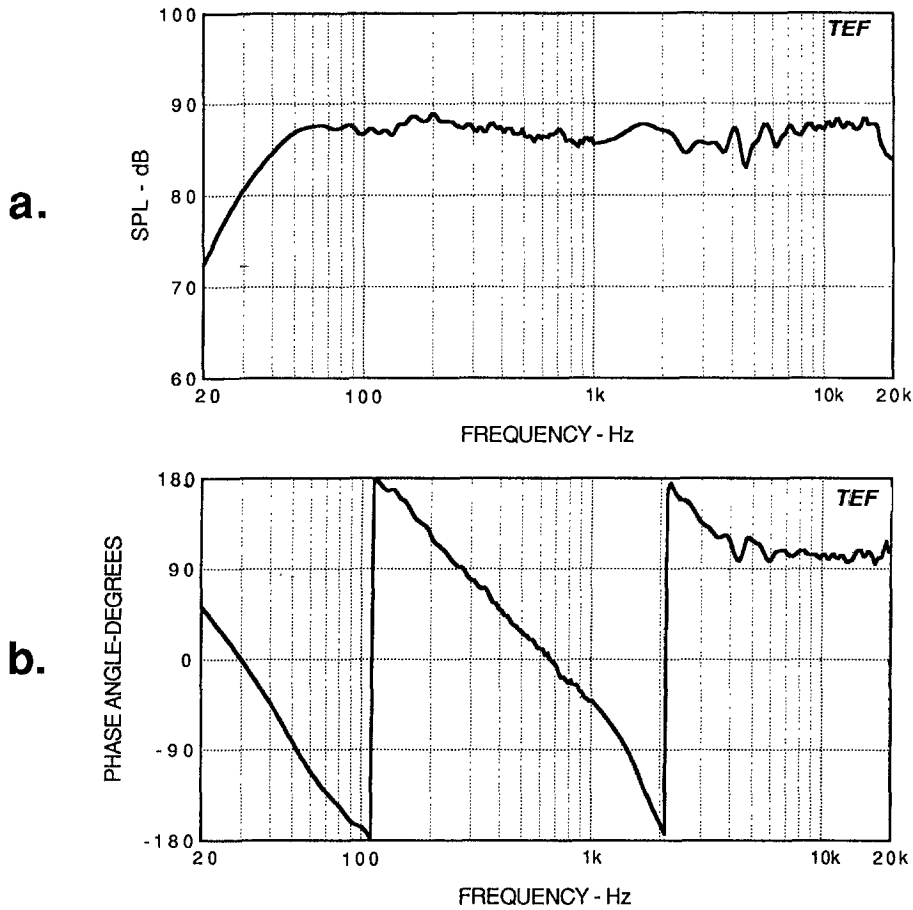

Fig. 14. Measured response curves for a three-way vented-box loudspeaker system composed of a 10-in. cone woofer, 6-in. cone midrange, and a 1-in. dome tweeter, plotted over the range of 20 Hz to 20 kHz. The system crossover frequencies are 250 Hz and 2.2 kHz. The lower crossover is an 18 dB/octave design, with an inverted polarity woofer, while the upper crossover is a 24 dB/octave Linkwitz-Riley design. (a) Magnitude vs frequency. (b) Phase vs frequency. (c) Group delay vs frequency. (d) Polarity phase vs frequency calculated using Eq. (4) and measured one-third-octave tone-burst data plotted with boxed data points. Also shown in (d) are octave-spaced filled-circle graphic symbols, taken from Fig. 2, that visually emphasize the polarity-phase variations with frequency. The wide variations of polarity phase indicates that this system will not preserve the phase of time-constrained narrow-band signals passed through it.

c.

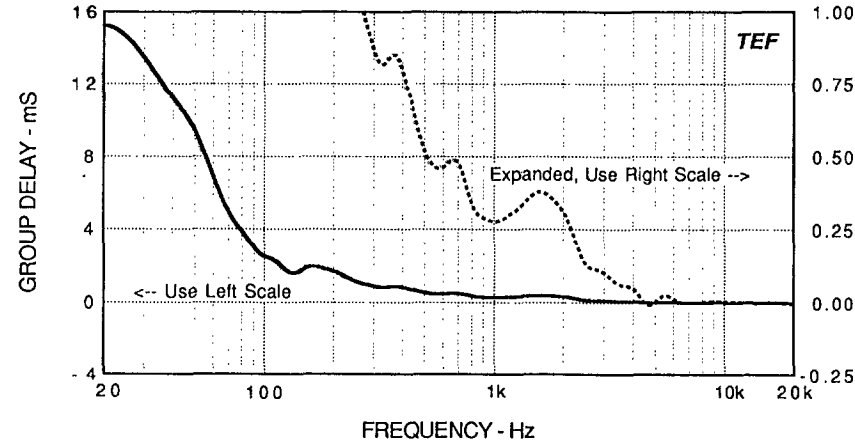

d.

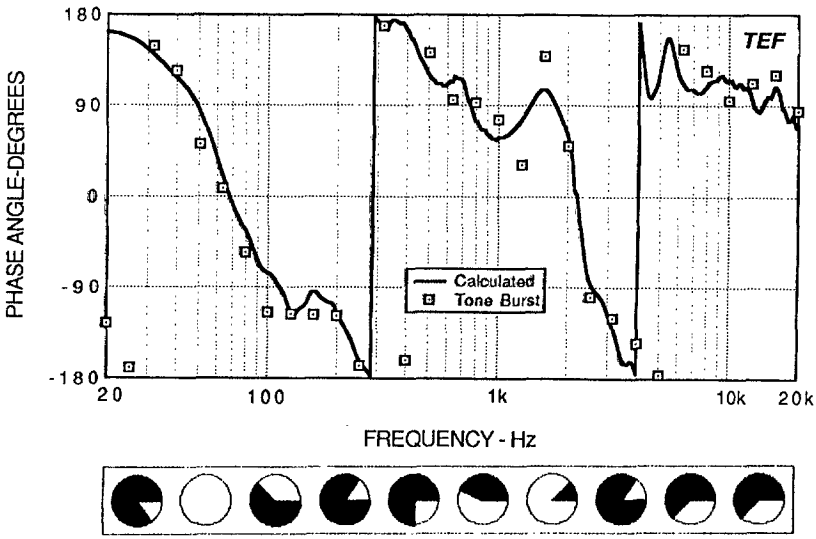

Fig. 14. Continued

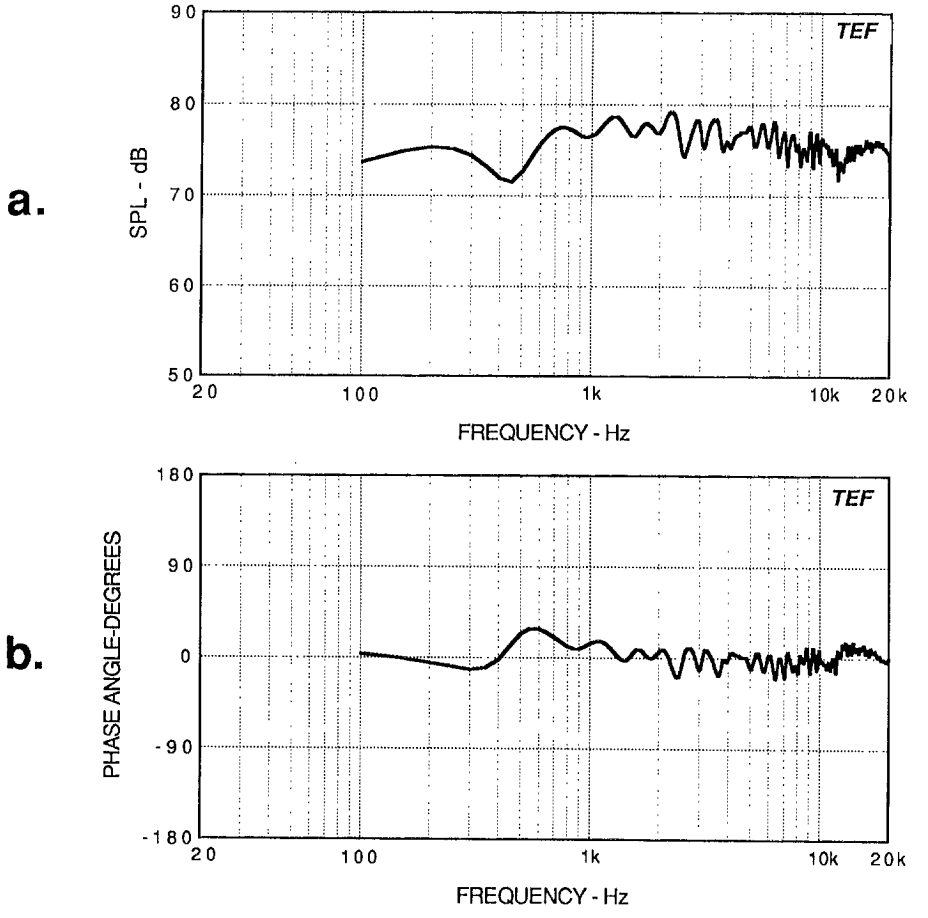

Fig. 15. Measured response curves for a very-expensive high-end five-way closed-box system designed for complete time and phase coherence, plotted over the range of 100 Hz to 20 kHz. The system uses three 8-in. cone woofers, 5-in. cone midrange, 2-in. dome upper-midrange, and a 1-in. dome tweeter. The crossover frequencies are at 50 Hz, 400 Hz, 1 kHz, and 3 kHz. The curves were measured in a live listening room using high selectivity TDS measurements, which essentially capture the direct sound only. Because of the high selectivity, the response below 500 Hz is questionable. (a) Magnitude vs frequency. (b) Phase vs frequency. (c) Group delay vs frequency. (d) Polarity phase vs frequency calculated using Eq. (4). Also shown in (d) are octave-spaced filled-circle graphic symbols, taken from Fig. 2, that visually emphasize the polarity-phase variations with frequency. Note the small variations in polarity phase (only about ±20°), which implies that the system will preserve the phase of time-constrained narrow-band signals it reproduces.

c.

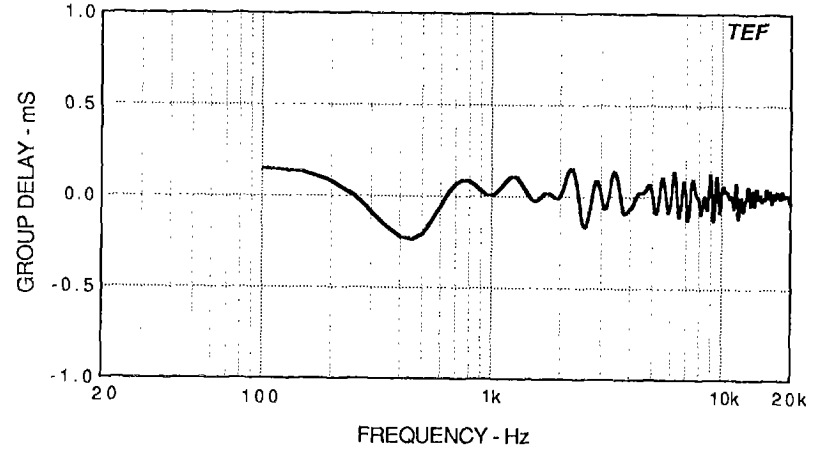

d.

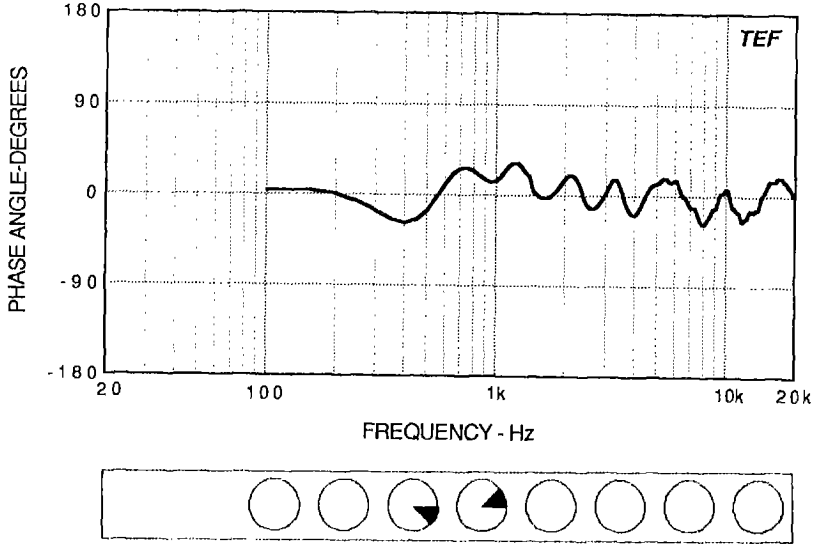

Fig. 15. Continued